

ELEVATION OF THE FATIGUE RESISTANCE OF THE JOINTS OF 7056-T351 ALUMINUM ALLOY OBTAINED BY ELECTRON-BEAM WELDING

V. M. Nesterenkov,¹ S. I. Motrunich,^{1,2} O. M. Berdnikova,¹
I. M. Klochkov,¹ and E. V. Polovetskyi¹

UDC: 621.791.722:539.431

We study welded joints of thermally hardened 7056-T351 aluminum alloy with elevated zinc content obtained by electron-beam welding (EBW) both in the intact state and after high-frequency mechanical impact treatment. It is shown that the process of EBW leads to the formation of a high-quality welded joint with high strength and fatigue-resistance characteristics. We determine the effective parameters of high-frequency mechanical impact treatment and analyze their influence on the microstructure, fracture behavior, and microhardness of the metal over the depth from the treated surface. In the course of hardening of the joint by high-frequency mechanical impact treatment, the grain structure becomes finer, the microhardness increases, and the character of fracture changes as a result of dispersion of elements of the microscopic topography of fracture surfaces.

Keywords: high-strength aluminum alloys, electron-beam welding, high-frequency mechanical sliding, microstructure, fatigue resistance.

Introduction

Thermally hardened aluminum alloys have high specific strength, corrosion resistance, and the characteristics of fatigue strength and fatigue crack-growth resistance. Therefore, they are suitable for manufacturing of the units of carrier rockets and spacecrafts, launching facilities, ships, air and land transport, agricultural machines, chemical equipment, and other welded structures operating, as a rule, under severe working conditions [1–3].

Thermally hardened high-strength aluminum alloys of the Al–Zn–Mg–Cu alloying system are now successfully applied in the production of aeronautical equipment [4]. As compared with 7150 and 7449 alloys, the developed 7056 aluminum alloy has improved characteristics of strength, corrosion resistance, and durability [5]. Note that mid- and large-sized components in the aircraft building and, in particular, the upper panels of wings operating under the conditions of cyclic loading are made from this alloy. The contemporary technological welding processes make it possible to reduce the mass of structures and, hence, decrease the costs of maintenance, i.e., guarantee the required characteristics of strength and durability [6–9]. The results of analysis of the characteristics of fatigue resistance of welded joints (WJ) of 7056 alloy are absent in the literature and, therefore, the investigations in this direction appear to be quite actual.

As a result of electron-beam welding (EBW) in a vacuum, due to the high concentration of energy in the electron beam, it is possible to obtain WJ with the minimum sizes of the heat-affected zone (HAZ) and high

¹ E. Paton Institute of Electric Welding, National Academy of Sciences of Ukraine, Kyiv, Ukraine.

² Corresponding author; e-mail: paton.testlab@gmail.com.

depth-to-width ratios [10]. In this case, it is possible to use low heat inputs with small volumes of melted metal in the bath and short-term thermal influence upon the welded metal. As a result of introduction of a small amount of heat into the product, its deformation sharply decreases. Welding in a vacuum prevents the saturation of melted metal heated by gases as a result of which we obtain high-quality WJ of chemically active metals and alloys [11].

By using the methods of surface plastic deformation (shot blasting, pneumatic peening, roll milling, ultrasonic impact treatment, or high-frequency mechanical peening) applied after welding and intended to relieve residual welding stresses, induce residual compressive stresses, and form fine-grained structures in the near-surface layers of the metal, it is possible to significantly increase the operating characteristics of welded joints [12–16]. It is known that the procedure of high-frequency mechanical impact (HFMI) treatment gives the maximum increase in the characteristics of fatigue strength of WJ of structural steels as compared with the other types of post-welding treatment [17–19].

In what follows, we study the structural features and mechanical properties under static and cyclic loads of the joints of 7056-T351 high-strength aluminum alloy obtained by the EBW procedure in the original state and after HFMI treatment.

Material and Methods

We tested specimens of butt WJ (30 mm in thickness) of 7056 high-strength aluminum alloy (8.5–9.7% Zn, 1.5–2.3 Mg, and 1.2–1.9 Cu) in the T351 thermally hardened state. The EBW procedure was carried out in a vacuum by using a computer-controlled UL-209M installation developed and produced at the E. Paton Institute of Electric Welding and equipped with a power complex formed by an ELA-60/60 high-voltage power supply and an electron-beam gun moving in a vacuum chamber with inner sizes of $3850 \times 2500 \times 2500$ mm. A working vacuum of $2.66 \cdot 10^{-4}$ mm Hg in the chamber and a vacuum of $5 \cdot 10^{-5}$ mm Hg in the gun were created for 30 min. The electron-beam gun with metallic tungsten cathode, together with the ELA-60/60 power supply, guarantees the realization of the range of electron-beam currents $I_b = 0\text{--}500$ mA for an accelerating voltage $U_{acc} = 60$ kV. For the development of the EBW technology for 7056-T351 alloy, the electron beam was subjected to local sweeping at a frequency of up to 1000 Hz with an amplitude of up to 4 mm.

The HFMI treatment of the welded joints of 7056-T351 alloys was realized with the use of an “USTREAT-500” device with a multirow seven-striker replaceable attachment with a diameter of strikers equal to 5 mm. The mechanical tests were carried out in an MTS 318.25 universal servohydraulic complex in agreement with the existing state standards. Cylindrical specimens with a diameter of 10 mm and a length-to-diameter ratio equal to 5 were manufactured from plates of the base metal of alloy with a thickness of 30 mm. These specimens were used to determine the initial mechanical characteristics of the alloy. Specimens with cross section 6×28 mm in size and a length of 250 mm used for the evaluation of the ultimate strength of the joint in uniaxial tension were made from welded plates $500 \times 250 \times 30$ mm in size with a central weld 500 mm in length.

To determine the fatigue strengths of the joints in the initial state and after hardening by the HFMI treatment, we cut out specimens $250 \times 6 \times 30$ mm in size. For the fatigue testing of the base metal (BM), we used corset-type specimens 250×30 mm in size (20 mm in the working zone). The investigations were carried out under the conditions of cyclic uniaxial tension at a frequency of 8 Hz for a loading ratio equal to 0.1.

The microstructure and specific features of the fracture of specimens were studied with the help of Versamet-2 and Neophot-32 optical microscopes and a Philips SEM-515 scanning electron microscope. The HV (1 N) microhardness of the metal was measured with the help of an M-400 instrument (Leco) under a load of 100 g, whereas the HV (0.5 N) microhardness was measured by using a PMT-3M device under a load of 50 g.

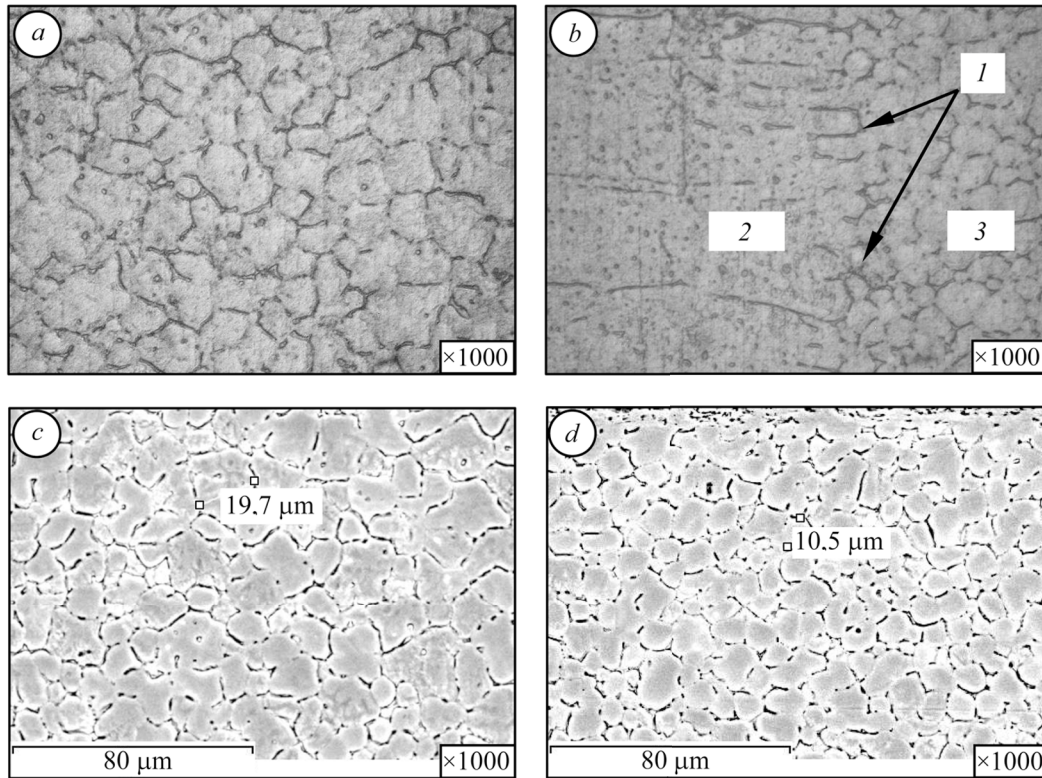


Fig. 1. Microstructure of the BM (a), FL (b), and the subsurface layer of the BM (c, d) for welded joints prepared by electron-beam welding (EBW) in the intact state (a–c) and after high-frequency mechanical impact (HFMI) treatment (d): (1) FL; (2) HAZ; (3) BM.

Table 1
Microhardness of the Zones of WJ in 7056-T351 Alloy

Zone	WM	FL		HAZ	BM
		WM	HAZ		
HV (1N), MPa	1360	1600–1870	1690–1760	1700	1560

Results and Discussion

Microstructure and Mechanical Properties. It was established that the weld metal (WM) has an equiaxial structure with a grain size of 4–20 μm without pores and cracks (Fig. 1a). The grain structure observed near the fusion line (FL) on the side of the weld remains almost invariant. At the same time, on the side of the HAZ, we observe the formation of a banded structure with bands 10–30 μm in width (Fig. 1b). The BM of 7056-T351 alloy has the structure with grains 6–10 μm in size and uniform directivity along the banded structure (with a width of up to 15 μm) formed under the conditions of directed deformation (forge rolling). The characteristics of microhardness of the WM are lower than for the BM by 13%. At the same time, in the zone of fusion, the microhardness is higher by 9–13% (Table 1).

Table 2
Mechanical Properties of the BM and WJ of 7056-T351 Alloy

Sample	σ_{UTS} , MPa	σ_{YS} , MPa	δ_5 , %
BM	610–625	540–560	14–16
WJ	412–426	–	–

Table 3
Variations of the HV (0.5 N) Microhardness over the Depth δ from the Surface of BM of the Joints of 7056-T351 Alloys after HFMI Treatment

δ , mm	HFMI Rate, mm ² /sec				
	without treatment	30	60	90	120
0	332–356	390–440	309–345	268–309	260–278
0.05	286–298	309–345	268–309	260–268	260
0.1	268–278	268–286	260–268	260	260
≥ 0.2	260	260–268	260	260	260

The ultimate strength σ_{UTS} for a batch of specimens (5 pieces) of WJ is equal to 412–426 MPa, i.e., ~ 70% of the corresponding characteristic for the BM (Table 2).

Prior to the HFMI treatment of WJ, we studied the variations of the characteristics of microhardness on specimens of the BM. This enabled us to evaluate the level of hardness of plastically deformed surface layers of the metal over the depth (δ) depending of the rate (productivity) of the process. It was established that the microhardness of the metal in the zone of peening increases as the rate of impact treatment decreases (Table 3). For a treatment rate of 60–120 mm²/sec, the microhardness of the subsurface layer of the metal is lower than for the metal in the intact state. As the rate of treatment decreases further (down to 30 mm²/sec), the microhardness of the plastically deformed surface layer of the metal in the zone of treatment increases by 20%.

This is why the central part of a sample of WJ was treated at a rate of 30 mm²/sec. We hardened a surface with an area of 1800 mm² containing the WM, HAZ, and BM. The microhardness was measured directly on the surface. It was established that, in the initial state, the microhardness of the WM is much lower than for the HAZ. After the HFMI treatment, the microhardnesses of the WM and HAZ substantially increased (Table 4). The HFMI procedure is accompanied by the refinement of the grain structure (Figs. 1c, d), which leads to its hardening. The increase in the level of microhardness observed as the grain size decreases is described by the Hall–Petch relation [20].

The fatigue limit for the samples of joints produced by EBW on a base of $2 \cdot 10^6$ cycles of stresses is equal to 141 MPa, which constitutes about 70% of the corresponding values for the BM (Fig. 2). At the same time, the fatigue life of specimens in the stage of crack propagation up to the final fracture is much shorter than in the stage of crack initiation, which is explained by the low plasticity of the WM and HAZ. The short-time fatigue

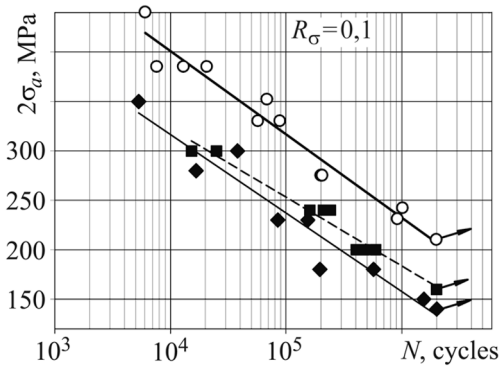


Fig. 2. Fatigue curves of the BM and WJ of 7056-T351 aluminum alloy: (○) BM; (◆) WJ in the intact state; (■) WJ hardened by the HFMI treatment.

Table 4
Microhardness of the Surface of WJ of 7056-T351 Aluminum Alloy
Prior to and After HFMI treatment

Specimen		Zone	
		WM	HAZ
Initial	HV (0.5N),	221–251	260–298
Hardened by HFMP	MPa	321–390	345–405

strength of the WJ after HFMI treatment is equal to 161 MPa, which constitutes 78% of its value for the BM (Fig. 2). At the same time, within the range 10^4 – $2 \cdot 10^6$ cycles, the fatigue life becomes 1.4–2 times longer than for the joints in the intact state.

Fractographic Investigations. The fracture processes in the zone of initiation of fatigue crack are mixed and transgranular, namely, quasibrittle (Fig. 3a) or brittle (Fig. 3b). The main fracture is mainly intergranular in the presence of secondary microcracks along the boundaries of the structural components (Fig. 3c). The size of facets of quasibrittle and brittle cleavage is equal to 8–20 μm , which corresponds to the grain sizes of the WM (see Fig. 1a). After the HFMI treatment, along the entire perimeter from the outer surface of the specimen, we recorded a zone of slow crack growth down to a depth of 30 μm (Fig. 3d) and the microscopic topography of the fracture surface was ductile. The main fracture is homogeneous and quasipitting with facets of 3–10 μm in size. The secondary cracks were not detected (Figs. 3e, f).

Thus, after the HFMI treatment of welded joints, the character of fracture changes from brittle to quasibrittle with a double decrease in the sizes of elements of the microscopic topography of the fracture surface. This structure guarantees an increase in the fatigue resistance of the WJ.

CONCLUSIONS

It is shown that the ultimate strength and fatigue limit of welded joints of 7056-T351 high-strength aluminum alloy prepared by EBW constitute ~70% of the values typical of the base metal. It was discovered that

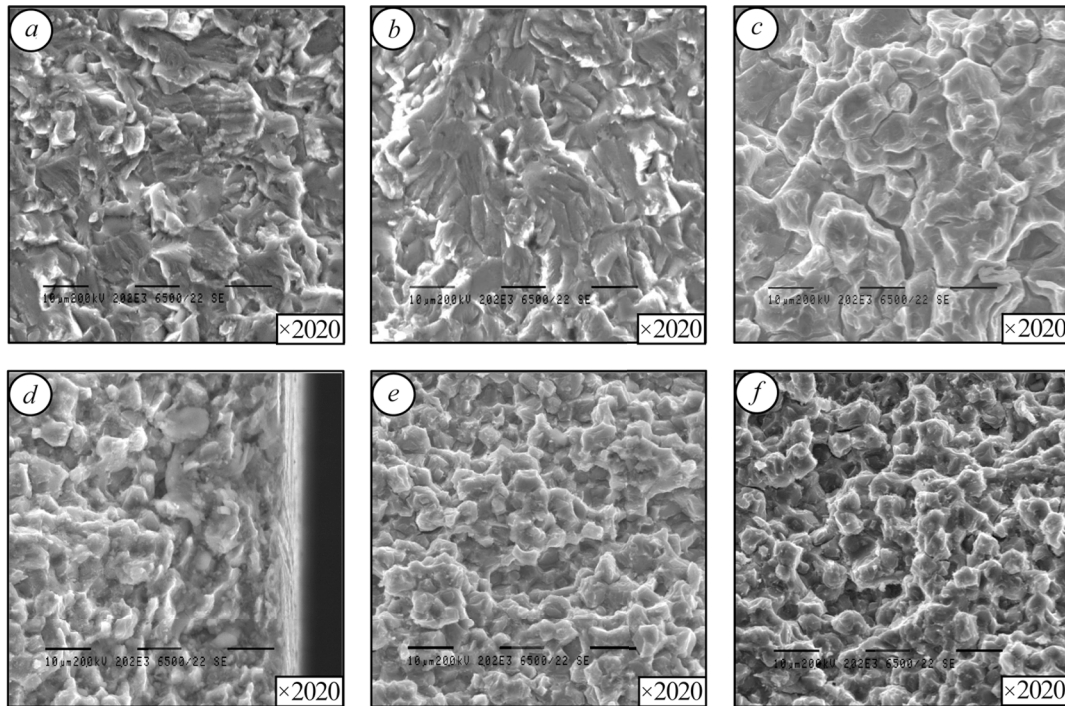


Fig. 3. Microfractograms of the WM of welded joints prepared by EBW in the initial state (a–c) and after HFMI treatment (d–f).

a defect-free uniform structure is formed in the weld metal, on the fusion line, and in the heat-affected zone. For the effective rate of the HFMI treatment ($30 \text{ mm}^2/\text{sec}$), the weld metal is hardened, which is accompanied by the refinement of structure and an increase in the microhardness. This post-welding technology of treatment of the WJ guarantees a 1.2–2-fold increase in the fatigue strength as compared with joints in the intact state within the loading range 10^4 – $2 \cdot 10^6$ cycles of stresses. The obtained results indicate that EBW is promising for getting joints of 7056-T351 alloy. Moreover, the HFMI technology can be recommended for increasing their fatigue life under cyclic loading.

REFERENCES

1. A. Ishchenko, "High-strength aluminum alloys for welded structures," *Progres. Mater. Tekhnol.*, **1**, 50–82 (2003).
2. M. A. Gureeva, O. E. Grushko, and V. V. Ovchinnikov, "Welded aluminum alloys in the structures of transport facilities," in: *VIAM/2008-205182* [in Russian], VIAM, Moscow (2008), pp. 51–82.
3. V. D. Shelyahin, A. V. Bernats'kyi, O. M. Berdnikova, V. M. Sydorets', O. V. Siora, and S. H. Hryhorenko, "Influence of the technological specific features of laser welding of titanium–aluminum structures on the structure formation in welded joints," *Metallofiz. Novit. Tekhnol.*, **42**, No. 3, 345–361 (2020).
4. A. Merati and G. Eastaugh, "Determination of fatigue related discontinuity state of 7000 series of aerospace aluminum alloys," *Eng. Failure Anal.*, **14**, No. 4, 673–685 (2007).
5. L. Zhou, K. Chen, S. Chen, X. Zhang, S. Fan, and L. Huang, "Comparison of hardenability and overaging precipitation behavior of three 7xxx aluminium alloys," *Mater. Sci. Technol.*, **35**, No. 6, 637–644 (2019).
6. M. Uthayakumar, V. Balasubramanian, A. M. A. Rani, and B. Hadzima, "Effects of welding on the fatigue behavior of commercial aluminum AA-1100 joints," *IOP Conf. Ser.: Mater. Sci. Eng.*, **346**, 1–12 (2017).
7. I. Klochkov, A. Poklaytsky, and S. Motrunich, "Fatigue behavior of high strength Al–Cu–Mg and Al–Cu–Li alloys joints obtained by fusion and solid state welding technologies," *J. Theor. Appl. Mech.*, **49**, 179–189 (2019).
8. A. Ya. Ishchenko, "Specific features of the application of high-strength aluminum alloys in welded structures," *Avtomat. Svarka*, **9**, 16–26 (2009).

9. L. I. Markashova, V. V. Arsenyuk, O. M. Berdnikova, and I. L. Bogajchuk, "Features of the phase formation in conditions of pressure welding of dissimilar materials at high-rate deforming," *Metallophys. Adv. Technol.*, **23**, No. 10, 1403–1417 (2001).
10. O. K. Nazarenko, V. M. Nesterenkov, and R. V. Ilyushenko, "Weldability of aircraft aluminium alloys of great thickness in EBW," *Paton Weld. J.*, **8**, 25–31 (2005).
11. G. Chen, J. Liu, S. Xi, B. Zhang, and J. Feng, "Study on microstructure and performance of molybdenum joint welded by electron beam," *Vacuum*, **154**, 1–5 (2018).
12. M. K. Kulekci and U. Esme, "Critical analysis of processes and apparatus for industrial surface peening technologies," *Int. J. Adv. Manuf. Technol.*, **74**, 1551–1565 (2014).
13. W. Pacquentin, N. Caron, and R. Oltra, "Effect of microstructure and chemical composition on localized corrosion resistance of a AISI 304L stainless steel after nanopulsed-laser surface melting," *Appl. Surf. Sci.*, **356**, 561–573 (2015).
14. T. Balusamy, T. S. N. Sankara Narayanan, and K. Ravichandran, Il, S. Park, and M.-H. Lee, "Influence of surface mechanical attrition treatment (SMAT) on the corrosion behavior of AISI 304 stainless steel," *Corros. Sci.*, **74**, 332–344 (2013).
15. B. Suyitno, T. D. Arifvianto, M. Widodo, P. Mahardika, and U. A. Dewo, "Salim effect of cold working and sandblasting on the microhardness, tensile strength, and corrosion resistance of AISI 316L stainless steel," *Int. J. Miner., Metall. Mater.*, **19**, 1093–1099 (2015).
16. L. I. Markashova, N. A. Pashchin, O. M. Berdnikova, O. Mikhodui, and Yu. M. Sidorenko, "Influence of impulsive electric current on the fine structure of AMg6 aluminum alloy subjected to electrodynamic treatment," *Mater. Sci.*, **54**, No. 1, 82–87 (2018).
17. L. M. Lobanov, V. I. Kirian, V. V. Knysh, and G. I. Prokopenko, "Improvement of fatigue resistance of welded joints in metal structures by high-frequency mechanical peening (Review)," *Paton Weld. J.*, **9**, 2–8 (2006).
18. H. C. Yildirim and G. B. Marquis, "Overview of fatigue data for high frequency mechanical impact treated welded joints," *Weld. World*, **56**, 82–96 (2012).
19. V. Knysh, S. Solovei, L. Nyrkova, I. Klochkov, and S. Motrunich, "Influence of the atmosphere corrosion on the fatigue life of welded T-joints treated by high frequency mechanical impact," *Proc. Struct. Integr.*, **16**, 73–80 (2019).
20. C. E. Carlton and P. J. Ferreira, "What is behind the inverse Hall-Petch effect in nanocrystalline materials?" *Acta Mater.*, **55**, 3749–3756 (2007).